Spatiotemporal pattern processing in a compartmental-model neuron

Paul C. Bressloff
GEC-Marconi Limited, Hirst Research Center, East Lane, Wembley, Middlesex HA9 7PP, England

John G. Taylor
Department of Mathematics, King's College, The Strand, London WC2R 2LS, England
(Received 9 September 1992; revised manuscript received 30 November 1992)

A neural-network model is constructed in which the activation state $V(t)$ of a neuron is of the general form $V(t)=\sum_j \int \chi_j(t,s)w_j a_j(s)ds$, where w_j is the weight of the jth input line, $a_j(s)$ is the input at time s, and χ_j is a response function that incorporates details concerning the passive membrane properties of dendrites. The response function is determined using a compartmental model of the dendrites. A simple analytical expression for χ_j is derived in the special case of an infinite uniform chain of compartments along similar lines to the analysis of diffusion on a one-dimensional lattice. This is then used to study the response of the model neuron to input patterns of specific spatial frequency across the chain. It is also shown how the inclusion of shunting effects results in the neuron's activation state being a nonlinear function of inputs, and that this provides a possible solution to the problem of high firing rates in neural-network models. Finally, perceptronlike learning in the model neuron is discussed, and the ability of the neuron to extract temporal features of an input signal is investigated.

PACS number(s): 87.10.+e, 02.50.−r, 05.20.−y

I. INTRODUCTION

Most models of a neuron used in artificial neural networks neglect the spatial structure of a neuron's extensive dendritic tree system. However, from a computational viewpoint there are a number of reasons for taking into account such structure: (i) The passive membrane properties of a neuron's dendritic tree leads to a spread of activity through the tree from the point of stimulation at a synapse. (Such a diffusive process can be described mathematically in terms of a cable equation [1,2]). Consequently, the time course of the membrane potential response at the soma induced by a synaptic input depends on the location of the synapse within the dendritic tree. For example, the response tends to rise more slowly and reaches a smaller peak the further away the synapse is from the soma (measured in terms of effective electronic distance). Hence spatial structure influences the temporal processing of synaptic inputs. (ii) The spatial relationship of synapses relative to each other and the soma is important. For example, an inhibitory synapse can effectively oppose the ability of a post-synaptic potential generated by more distal excitatory synapses to spread to the soma. On the other hand, an inhibitory synapse has little effect on more proximal excitatory synapses. One possible computational role of such a feature is a logical AND-NOT operation—this has been suggested as providing a mechanism for directional selectivity in retinal ganglion cells [3]. (iii) The geometry of the dendritic tree ensures that different branches can function almost independently of one another. Moreover, there is growing evidence that the presence of voltage-dependent gates can confer excitable properties onto local branches such that the results of local computations can be transmitted effectively by generation of an action potential within the branch [4]. This suggests that quite complex computations are being performed within the dendrites prior to subsequent processing at the soma [5].

In this paper, we construct a neural-network model that takes into account the first of the above issues, that is, the effects of the passive membrane properties of dendrites on the processing of synaptic inputs. We shall consider, in particular, a model neuron whose activation state (approximating the membrane potential at the soma) is of the general form $V(t)=\sum_j \int \chi_j(t,s)w_j a_j(s)ds$, where w_j is the weight of the jth input line, $a_j(s)$ is the input at time s, and χ_j is a response function that incorporates details concerning the dendrites. We derive a general expression for χ_j by analyzing a compartmental model of the electrical properties of the dendrites [6,7], and then use this to study the response of the model neuron to spatiotemporal input patterns.

Compartmental models replace the partial differential equation of cable theory [1,2], which describes the current flow in a continuous passive dendritic tree, by a set of coupled ordinary differential equations. This is achieved by dividing the continuously distributed system into sufficiently small regions or compartments such that the spatial variations of the membrane potential within a region are negligible, as are fluctuations in specific electrical properties, cable diameter, etc. Each such isopotential region is coupled by Ohmic resistors to its immediate neighbors; the nonuniformity in physical properties and differences in membrane potential occur between compartments. Moreover, the topology of the connections between compartments may be used to represent the complex dendritic tree structure. The usefulness of the compartmental approach is that, in the case of nontrivial models, it leads to a simpler and less computationally expensive treatment of dendritic structure than cable

theory. Indeed, compartmental models form the basis of most computer simulations of neurons [7]. It should be stressed, however, that all of the results presented in this paper concerning the response of our model neuron to synaptic input patterns can be derived equally well in terms of either compartmental or cable formulations of the passive membrane properties of dendrites. We choose the former for convenience, and because it provides a platform for the study of more complex models.

The organization of the paper is as follows. Our general model of a neuron is constructed in Sec. II. A major assumption of the model is that active processes associated with voltage-dependent gates, such as those involved in the generation of action potentials, are ignored. For then the compartmental model equations are linear in the membrane potentials and can be integrated directly to determine χ_j. The resulting expression for χ_j applies to arbitrary topologies and to time-varying synaptic inputs with shunting; in the latter case, χ_j is expressed in terms of a time-ordered path integral.

The simple case of an infinite one-dimensional chain of compartments without shunting is studied in Sec. III. An analytical expression for χ_j is derived along similar lines to the study of diffusion on a one-dimensional lattice. This is used to investigate the response of the model neuron to input patterns of specific spatial frequency across the chain. We also indicate how the corresponding results for an infinite cable may be obtained in the continuum limit. We then study shunting effects in Sec. IV, analyzing the time-ordered path integral in a number of special cases. We show how shunting leads to a nonlinear relationship between the activation state of the neuron and its inputs, and use this to provide a solution to the problem of high firing rates that plagues a number of neural-network models. (An analogous result has been obtained by Abbott, who considers solutions to the stationary cable equations [8].) Finally, in Sec. V we extend recent work on temporal processing in time-summating neurons [9] to show how the model neuron is able to extract temporal features of an input sequence, such as the ordering of patterns within a sequence. We construct a perceptronlike learning rule and convergence theorem and illustrate how the incorporation of dendritic structure can enhance the performance of the neuron.

II. COMPARTMENTAL MODEL NEURON

A compartmental model [6,7] represents an unbranched cylindrical region of a passive dendritic membrane in terms of a linked chain of equivalent circuits as shown in Fig. 1. The equivalent circuit of the αth compartment consists of a membrane leakage resistor R_α in parallel with a capacitor C_α, with the ground representing the extracellular medium (assumed to be an isopotential). The electrical potential V_α across the membrane is measured with respect to the resting potential, i.e., the potential when there is no current flowing across the membrane. (A nonzero resting potential may be incorporated by placing a battery in series with the membrane resistor.) The compartment is joined to its immediate neighbors in the chain by the junctional resistors $R_{\alpha\alpha-1}$

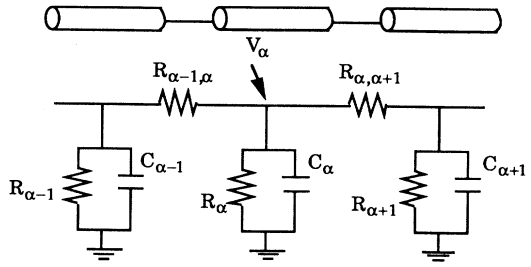

FIG. 1. Equivalent circuit for a compartmental model of a chain of successive cylindrical segments of passive dendritic membrane.

and $R_{\alpha\alpha+1}$. The time evolution of the membrane potential is determined by Kirchoff's law: For each compartment, the total current through the membrane is equal to the difference between the longitudinal currents entering and leaving that compartment. Thus,

$$C_\alpha \frac{dV_\alpha}{dt} = -\frac{V_\alpha}{R_\alpha} + \sum_{\langle\beta;\alpha\rangle} \frac{V_\beta - V_\alpha}{R_{\alpha\beta}} + I_\alpha \ , \tag{2.1}$$

where I_α represents any external currents injected into the region (via electrodes, for example), and $\langle\beta;\alpha\rangle$ indicates that the summation over β is restricted to immediate neighbors of α.

It is useful to relate the various parameters of the compartmental model to the electrical and physical properties of the underlying cylindrical region of the dendrite. Suppose that the cylinder has a uniform diameter d and denote the length of the αth compartment by l_α. Then

$$C_\alpha = c_\alpha l_\alpha \pi d \ , \quad R_\alpha = \frac{l}{g_\alpha l_\alpha \pi d} \ , \quad R_{\alpha\beta} = \frac{r_\alpha l_\alpha + r_\beta l_\beta}{2} \ , \tag{2.2}$$

where g_α and c_α are, respectively, the membrane conductance and capacitance per unit area, and r_α is the longitudinal resistance per unit length of cylinder, i.e., $r_\alpha = 4\rho_\alpha/\pi d^2$ with ρ_α the resistivity. The junctional resistance $R_{\alpha\beta}$ is taken to be the average of the longitudinal resistances of the neighboring compartments α and β.

In the continuum limit, Eq. (2.1) reduces to the partial differential equation of cable theory [1]. To show this, consider a uniform cylindrical region of dendrite that is partitioned into a chain of infinitesimal compartments, each labeled by its position x along the cylinder with $c_x = c$, $g_x = g$, $r_x = r$ for all x. Let the incremental length of each compartment be equal to δx. Taking the continuum limit $\delta x \to 0$, we then obtain from (2.1) and (2.2) the cable equation

$$\bar{\tau}\frac{\partial V}{\partial t} = -V(x) + \lambda^2 \frac{\partial^2 V}{\partial x^2} \tag{2.3}$$

for zero external current, where $\bar{\tau} = c/g$, $\lambda^{-2} = rg\pi d$, and λ is the characteristic length of the cable. The cable equation (2.3) describes current flow in a continuous passive dendrite. It has straightforward analytical solutions,

in the case of constant applied currents, to the steady states of an idealized class of dendritic trees that are equivalent to unbranched cylinders [1]. However, the solutions are considerably more complicated for nonuniform dendritic trees with a general branching structure, and for the spatiotemporal inputs associated with synaptic currents. In such cases, it is simpler and less computationally expensive to use a compartmental model.

The more complex geometry of a dendritic tree may be incorporated into Eq. (2.1) by an appropriate choice of the topology of the connections between compartments, as specified by the graph Γ, whose vertices are the compartmental labels α. Each branch of the tree is represented by a chain of compartments, and each branch point by a compartment with three, rather than two, nearest neighbors. The compartments of the two daughter branches will generally have different properties (leakage capacitance and resistance, etc.) from those of the parent branch. However, as shown by Rall [1], when certain conditions are satisfied concerning the relationship between parent and daughter branches, a dendritic tree is equivalent to an unbranched cylinder. For simplicity, we shall represent the geometry of the dendrites by a one-dimensional chain of $2M+1$ compartments labeled $\alpha=0,\pm1,\ldots,\pm M$; we shall illustrate in Sec. III how this simple structure is sufficient to capture the essential feature concerning the effects of the passive membrane properties of dendrites. (Note, however that if one is concerned with other aspects of dendritic computation as detailed in the Introduction, then one would need to consider more complex geometries.)

The compartmental model of Eq. (2.1) may also be easily modified to take into account synaptic currents. The arrival of an action potential at a synapse causes a depolarization of the presynaptic cell membrane resulting in the release of packets of neurotransmitters. The binding of these neurotransmitters to receptors on the postsynaptic cell membrane leads to the opening of channels allowing ions (Na^+, K^+, Cl^-) to move in and out of the cell under the influence of concentration and potential gradients [5]. The ionic membrane current is governed by a time-varying conductance Δg, which is in series with a reversal potential S whose value depends on the particular set of ions involved. The effective equivalent circuit for a compartment with a single synaptic input is shown in Fig. 2. Let $\Delta g_{\alpha k}$ and $S_{\alpha k}$ denote, respectively, the increase in synaptic conductance and the membrane reversal potential associated with the kth synapse of compartment α. For a compartment with N synaptic inputs, Eq. (2.1) becomes

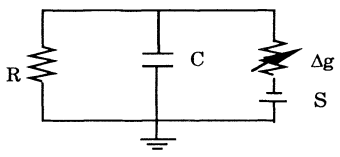

FIG. 2. Equivalent circuit for a compartment that receives a single synaptic input. S is the membrane reversal potential and Δg describes the change in conductance.

$$C_\alpha \frac{dV_\alpha}{dt} = -\frac{V_\alpha}{R_\alpha} + \sum_{\langle\beta;\alpha\rangle} \frac{V_\beta - V_\alpha}{R_{\alpha\beta}} + \sum_{k=1}^{N} \Delta g_{\alpha k}(S_{\alpha k} - V_\alpha) \, . \tag{2.4}$$

Since $\Delta g_{\alpha k}$ is positive, the effect of each term $\Delta g_{\alpha k}(S_{\alpha k}-V_\alpha)$ is for V_α to tend towards $S_{\alpha k}$. Hence positive and negative $S_{\alpha k}$ correspond, respectively, to excitatory and inhibitory synapses. (For convenience, all compartments are assumed to have the same number of synapses.)

Our major assumption concerning the synaptic inputs is that the conductance changes $\Delta g_{\alpha k}$ are *voltage independent*. That is, we ignore active processes such as those associated with the generation of an action potential, so that

$$\Delta g_{\alpha k}(t) = \epsilon_{\alpha k} x_{\alpha k}(t) \, , \tag{2.5}$$

where $\epsilon_{\alpha k}$ is a constant determined by factors such as the amount of neurotransmitter released on arrival of an action potential and the efficiency with which these neurotransmitters bind to receptors [11], and $x_{\alpha k}(t)$ is the arrival frequency of action potentials. Since $\Delta g_{\alpha k}$ is independent of the membrane potentials $\mathbf{V}=(V_{-M},\ldots,V_M)$, Eq. (2.4) may be written as a linear matrix equation of the form [10,11]

$$\frac{d\mathbf{V}}{dt} = \mathbf{H}(t)\mathbf{V}(t) + \mathbf{U}(t) \, , \quad H_{\alpha\beta}(t) = Q_{\alpha\beta} + \bar{Q}_{\alpha\beta}(t) \, , \tag{2.6}$$

where

$$Q_{\alpha\beta} = -\frac{\delta_{\alpha,\beta}}{\tau_\alpha} + \frac{\delta_{\beta,\alpha+1}}{\tau_{\alpha\alpha+1}}(1-\delta_{\alpha,M}) + \frac{\delta_{\beta,\alpha-1}}{\tau_{\alpha\alpha-1}}(1-\delta_{\alpha,-M}) \, , \tag{2.7}$$

$$\frac{1}{\tau_\alpha} = \frac{1}{C_\alpha}\left[\sum_{\langle\beta';\alpha\rangle}\frac{1}{R_{\alpha\beta'}} + \frac{1}{R_\alpha}\right] \, , \quad \frac{1}{\tau_{\alpha\beta}} = \frac{1}{C_\alpha R_{\alpha\beta}} \, , \tag{2.8}$$

$$\bar{Q}_{\alpha\beta}(t) = -\frac{\delta_{\alpha\beta}}{C_\alpha}\sum_k \Delta g_{\alpha k}(t) \, , \quad U_\alpha(t) = \frac{1}{C_\alpha}\sum_k \Delta g_{\alpha k}(t) S_{\alpha k} \, . \tag{2.9}$$

Formally, Eq. (2.6) may be solved as

$$\mathbf{V}(t) = \int_0^t dt' \mathbf{T}\left[\exp\left[\int_{t'}^t dt'' \mathbf{H}(t'')\right]\right]\mathbf{U}(t') + \mathbf{T}\left[\exp\left[\int_0^t dt'' \mathbf{H}(t'')\right]\right]\mathbf{V}(0) \, , \tag{2.10}$$

where $\mathbf{T}$ denotes the time-ordered product, $\mathbf{T}[\mathbf{H}(t)\mathbf{H}(t')] = \mathbf{H}(t)\mathbf{H}(t')\Theta(t-t') + \mathbf{H}(t')\mathbf{H}(t)\Theta(t'-t)$, where $\mathbf{H}$ is a time-dependent, noncommuting matrix. The term

$$\mathbf{T}\left[\exp\left[\int_{t'}^t dt'' \mathbf{H}(t'')\right]\right]_{\alpha\beta}$$

is the response function $\chi(\alpha,t;\beta,t')$ of the system.

In general, Eq. (2.10) is difficult to solve due to the dependence of χ on the synaptic inputs through the term

$\bar{Q}$ of Eq. (2.9). However, if the time-dependent part of $\mathbf{H}$ is absent, which corresponds to dropping the shunting term $-V_\alpha \sum_k \Delta g_{\alpha k}$ from Eq. (2.1), then

$$\mathbf{V}(t)=\int_0^t dt' e^{(t-t')\mathbf{Q}}\mathbf{U}(t')+e^{t\mathbf{Q}}\mathbf{V}(0) , \tag{2.11}$$

and $\chi(\alpha,t;\beta,t')$ reduces to the simpler form $(e^{(t-t')\mathbf{Q}})_{\alpha\beta}$. For the moment, we shall use Eq. (2.11) to model the effects of passive dendrites, returning to the more general expression (2.10) when we consider shunting in Sec. IV.

In order to construct our model of a neuron, it is necessary to supplement our description of the dendrites with details concerning the firing mechanism of a neuron. The latter involves a complex interaction between ionic currents and voltage-dependent gates at the axon hillock of the soma [5]. Such active processes may be incorporated into a compartmental model that takes into account the spatial structure of the soma in addition to that of the dendrites. However, for the purposes of this paper, we shall simply view the soma as a point processor that is isopotential with the dendritic compartment nearest to it, which is chosen to be at the center of the chain ($\alpha=0$) rather than at one end of the chain ($\alpha=\pm M$) as in Ref. [8], (see Fig. 3). This particular choice allows us to ignore end effects in the infinite chain limit, which greatly simplifies the analysis without losing important details concerning the passive membrane effects of dendrites; see Sec. III. At the simplest level of modeling, we can take the soma to be a binary-threshold device along the lines of the McCulloch-Pitts neuron [12]. That is, the neuron fires whenever the membrane potential at the soma, denoted by the *activation state* $V(t)$, exceeds a threshold h, and provided that the neuron is outside its absolute refractory period t_R. The firing times of the neuron satisfy the iterative equation

$$T_n=\inf\{t|V(t)\geq h;t\geq T_{n-1}+t_R\} , \tag{2.12}$$

where T_n is the time at which the neuron fires for the nth occasion since $t=0$.

There are a number of refinements of this simple model. For example, one can incorporate the effects of the *relative refractory period* by introducing a time-dependent threshold of the form $h(\Delta t)$, where Δt is the time after emission of the last action potential, such that $h(\Delta t)=\infty$ for $0<\Delta t\leq t_R$ and $h(\Delta t)$ is continuous and monotonically decreasing for $\Delta t>t_R$ (until the neuron fires again), e.g., $h(\Delta t)=h_0+h_1\exp(-\Delta t/\tau_a)$ for $\Delta T>t_R$, where $h_{0,1}$ and τ_a are constants. As shown by Amari [13], if $V(t)$ is slowly varying, then one can approximate the instantaneous firing rate $f(t)$ of the neuron by a sigmoid function,

$$f(t)=\frac{f_{\max}}{1+e^{-g[V(t)-\kappa]}} , \tag{2.13}$$

for some gain g and threshold κ. Equation (2.13) reflects the fact that the larger $V(t)$, the faster the decreasing threshold $h(\Delta t)$ is crossed from below and thus the greater the firing rate f. The maximum firing rate $f_{\max}$ is determined by the absolute refractory period. Another refinement is to take into account, *reset*. When a neuron fires, there is a rapid depolarization of the membrane potential at the axon hillock, followed by a hyperpolarization due to delayed rectifier potassium currents [5]. This process is often modeled by assuming that the membrane potential at the soma is reset to zero, $V(t)=0$, whenever the neuron fires— *integrate-and-fire models* [14]. We shall consider this further below.

If we now combine Eqs. (2.5), (2.9), and (2.11) we find that, in the absence of shunting, the activation state $V(t)$ is given by

$$\begin{aligned} V(t)&=\int_0^t ds \sum_{\alpha=-M}^{M}\chi_\alpha(t-s)\mathbf{w}_\alpha\cdot\mathbf{x}_\alpha(s) , \\ \mathbf{w}_\alpha\cdot\mathbf{x}_\alpha(s)&=\sum_{k=1}^{N} w_{\alpha k}x_{\alpha k}(s) , \end{aligned} \tag{2.14}$$

where $w_{\alpha k}=S_{\alpha k}\epsilon_{\alpha k}/C_\alpha$ and $\chi_\alpha(t-s)\equiv\chi(0,t;\alpha,s)=[\exp(t-s)\mathbf{Q}]_{0\alpha}$. In order to eliminate any reference to the compartmental membrane potentials V_α, $\alpha\neq 0$, we have omitted the transient term $\exp(t\mathbf{Q})\mathbf{V}(0)$ from Eq. (2.11); this is valid provided that we impose the initial condition $\mathbf{V}(0)=0$ or assume that t is sufficiently large so that all transients have decayed away. Thus we have arrived at the standard form for a neural-network model of a neuron [15], with the additional feature that information concerning the spatially distributed dendrites is encapsulated within the response function or kernel χ_α. In particular, the neuron can be viewed as a point processor (Fig. 4) whose mode of operation is to perform a linear summation of inputs, given by the activation state $V(t)$ of Eq. (2.14), and then to produce an output $y(t)=f(V(t))$, where f is some nonlinear function such as the sigmoid function of Eq. (2.13). The $(2M+1)N$ weights $w_{\alpha k}$ are arranged into $2M+1$ groups, labeled by α, that correspond to the $2M+1$ compartments of the dendritic chain.

We end this section by discussing how our model neuron is modified when reset is taken into account. First, note that we must replace Eq. (2.11) by

$$\begin{aligned} &\mathbf{V}(t)=\int_{T_n}^t dt' e^{(t-t')\mathbf{Q}}\mathbf{U}(t')+e^{(t-T_n)\mathbf{Q}}\mathbf{V}(T_n^+) , \\ &T_n\leq t<T_{n+1} , \end{aligned} \tag{2.15}$$

where T_n and T_{n+1} are consecutive firing-times of the neuron and $\mathbf{V}(T_n^+)$ is the value of the membrane potentials immediately after the neuron fires at time T_n. Since we are interested in eliminating the compartmental membrane potentials V_α, $\alpha\neq 0$, we impose the reset condition $V_\alpha(T_n^+)=0$ for all α. That is, we assume that the whole

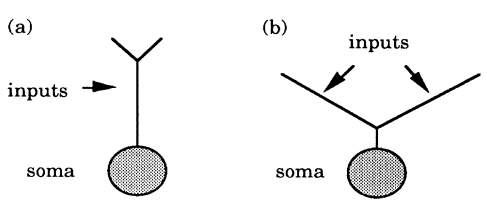

FIG. 3. Idealized dendritic tree with (a) soma located at one end of tree and (b) soma located at center of tree.

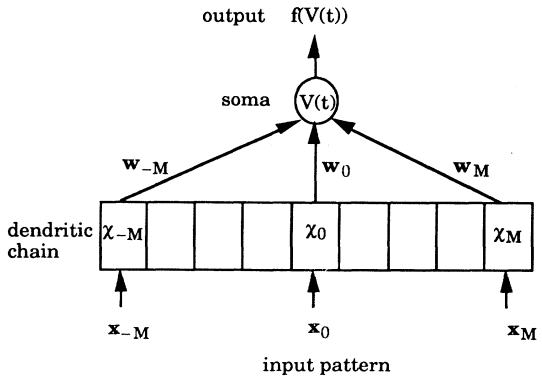

FIG. 4. Compartmental model of a neuron. Dendritic tree is represented as an idealized chain of $2M+1$ compartments. The activation state of the neuron is $V(t)$. The input pattern presented to the neuron is $\mathbf{x}=(\mathbf{x}_{-M},\ldots,\mathbf{x}_M)$, where $\mathbf{x}_\alpha=(x_{\alpha 1},\ldots,x_{\alpha N})$. The corresponding weights are $\mathbf{w}=(\mathbf{w}_{-M},\ldots,\mathbf{w}_M)$. The input $\mathbf{x}_\alpha$ to each compartment is convolved with the response function χ_α.

neuron resets its membrane potential after firing. (A more realistic picture is that the spread of activity induced by a neuron firing is such that the effects of reset decrease as one proceeds distally from the soma; see also comments at the end of Sec. V.) Under such an assumption, the analogue of Eq. (2.14) in the presence of rest is

$$V(t)=\int_{T_n}^{t} ds \sum_{\alpha=-M}^{M} \chi_\alpha(t-s)\mathbf{w}_\alpha\cdot\mathbf{x}_\alpha(s) , \tag{2.16}$$

with

$$V(T_{n+1}^{+})=0 \quad \text{if} \quad V(T_{n+1})=h , \tag{2.17}$$

where h is the threshold.

III. INFINITE ONE-DIMENSIONAL DENDRITIC CHAIN

In this section, we shall determine $\exp(t\mathbf{Q})$ in the special case of a uniform, infinite dendritic chain, and then analyze the output response of the model neuron satisfying (2.14) or (2.16). First note that the matrix $\mathbf{Q}$ has real, negative, nondegenerate eigenvalues $-\lambda_i$ (for any topology), i.e., $\lambda_i>0$ and $\lambda_i\neq\lambda_j$ for $i\neq j$. This reflects the fact that $\mathbf{Q}$ determines the time evolution of membrane potentials in a passive RC circuit, which is a dissipative system. It follows from standard linear analysis that [10]

$$\chi(\alpha,t;\beta,s)=(e^{(t-s)\mathbf{Q}})_{\alpha\beta}=\sum_i e^{-(t-s)\lambda_i}C^i_{\alpha\beta} . \tag{3.1}$$

However, a more explicit expression for $\exp(t\mathbf{Q})$ can be derived in the special case of a uniform chain of dendritic compartments in the limit $M\to\infty$, since familiar results from the study of classical diffusion on a one-dimensional lattice may then be used. (In the case of an infinite dendritic chain, we no longer have to worry about edge effects arising from the compartments at $\pm M$.) Setting $R_\alpha=R$, $C_\alpha=C$, $R_{\alpha\alpha+1}=\tilde{R}$ for all α, Eqs. (2.7) and (2.8) give

$$\begin{aligned} Q_{\alpha\beta}&=-\frac{\delta_{\alpha,\beta}}{\tau}+\frac{\delta_{\beta,\alpha+1}}{\gamma}+\frac{\delta_{\beta,\alpha-1}}{\gamma} ,\\ \frac{1}{\tau}&=\frac{2}{\gamma}+\frac{1}{\bar{\tau}} ,\\ \gamma&=\tilde{R}C ,\\ \bar{\tau}&=RC . \end{aligned} \tag{3.2}$$

For identical compartments, the diagonal part of $\mathbf{Q}$ gives a global factor $\exp(-t/\tau)$ in Eq. (3.1). Moreover, using the fact that the off-diagonal terms in $\mathbf{Q}$, Eq. (3.2), link adjacent elements of the chain, we find that in the limit $M\to\infty$, the response function satisfies $\chi(\alpha,t;\beta,s)=\chi(\alpha-\beta,t-s)$, with

$$\chi(\alpha-\beta,t)=\left[\frac{t}{\gamma}\right]^{|\beta-\alpha|}e^{-t/\tau} \times\sum_{p\geq 0}\left[\frac{t}{\gamma}\right]^{2p}\frac{N_{|\beta-\alpha|+2p}[\beta,\alpha]}{(|\beta-\alpha|+2p)!} , \tag{3.3}$$

where $N_q[\beta,\alpha]$ is the number of possible paths that can be taken by a random walk consisting of q steps of unit length from point β to point α. Using the result that [16]

$$N_q[\beta,\alpha]=\begin{pmatrix} q \\ [q+|\beta-\alpha|]/2 \end{pmatrix}$$

Eq. (3.3) becomes

$$\begin{aligned}\chi(\alpha-\beta,t)&=\left[\frac{t}{\gamma}\right]^{|\beta-\alpha|}e^{-t/\tau}\sum_{p\geq 0}\left[\frac{t}{\gamma}\right]^{2p}\frac{1}{(|\beta-\alpha|+p)/!p!}\\ &=e^{-t/\tau}I_{|\alpha-\beta|}(2t/\gamma) ,\end{aligned} \tag{3.4}$$

where I_n is the modified Bessel function of integer order.

The function $\chi(L,t)$, $L>0$ describes the response at time t of a compartment in an infinite dendritic chain to an impulse at $t=0$ impinging on another compartment separated from the first by a distance L along the chain. In Fig. 5, $\chi(L,t)$ is plotted as a function of t/γ for a range of L values with $\bar{\tau}=5.0\gamma$. For compartments near the point of stimulation β, there is a sharp rise to a larger peak followed by a rapid early decay, while compartments far from β exhibit a slower rise to a later and more rounded peak. Suppose that we neglect all but the first term of the sum on the right-hand side of (3.4). Then χ reduces to the response function recently used in the so-called gamma model of a neuron [17],

$$\begin{aligned}\chi(L,t)&\approx\frac{e^{-t/\tau}}{L!}\left[\frac{t}{\gamma}\right]^{L} ,\\ \frac{d\chi}{dt}(L,t/\gamma)&\approx e^{-t/\tau}\left[\frac{t}{\gamma}\right]^{L-1}\frac{L-t/\tau}{L!} .\end{aligned} \tag{3.5}$$

In this particular case, the maximum response occurs at $t_d\approx L\tau$, i.e., the response time t_d increases linearly with the distance L between the point of stimulation β and the

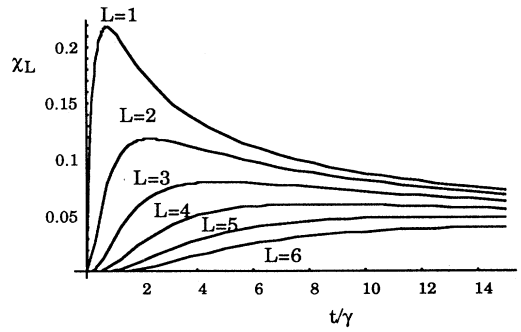

FIG. 5. Response function χ_L of an infinite dendritic chain plotted against time t (in units of γ) for different values of the distance L along the chain between the soma and the point of stimulation.

compartment α. Moreover,

$$\chi_L^{\max} \approx \left[\frac{L\tau}{\gamma}\right]^L \frac{e^{-L}}{L!} , \tag{3.6}$$

i.e., the maximum effect is reduced exponentially with the distance along the chain from the point of stimulation. Returning to Fig. 5, we note that the response curves are similar to those found in more realistic models of neurons [6,7]. In other words, the effects of passive membrane properties of dendrites on the behavior of a neuron can be captured using the simple response function of a uniform, infinite dendritic chain.

Having obtained the response function of a uniform chain, we can now determine the output response of our model neuron satisfying (2.14). Setting $\chi_\alpha(t)=\chi(\alpha,t)$ and using Eq. (3.4), we have

$$V(t)=\int_0^t ds \sum_{\alpha=-\infty}^{\infty} e^{-(t-s)/\tau} I_{|\alpha|}(2(t-s)/\gamma)\mathbf{w}_\alpha\cdot\mathbf{x}_\alpha(s) . \tag{3.7}$$

As an example, suppose that the neuron receives an input stimulation consisting of a sequence of impulse patterns of the form

$$\mathbf{w}_\alpha\cdot\mathbf{x}_\alpha(t)=\sum_{m=0}^{2} u_\alpha(m)\delta(t-2m) . \tag{3.8}$$

(Each impulse corresponds to an idealized action potential spike; see Sec. IV.) Consider, in particular, the two sequences A-B-C and C-B-A shown in Fig. 6. The former sequence consists of a local stimulation of the dendritic chain that proceeds from a proximal to a distal location along the positive half of the chain relative to the soma at $\beta=0$. That is, $u_\beta(0)=I(\delta_{\beta,1}+\delta_{\beta,2})$, $u_\beta(1)=I(\delta_{\beta,3}+\delta_{\beta,4})$ and $u_\beta(2)=I(\delta_{\beta,5}+\delta_{\beta,6})$, respectively, where I is the amplitude of each impulse. In the latter sequence, the simulation proceeds in the opposite direction.

The activation state of the neuron induced by each of these sequences is illustrated in Fig. 7. It can be seen that the sequence C-B-A produces a delayed rise to a larger peak amplitude. (Such behavior is very similar to that found in detailed computer simulations of neurons (cf. Fig. 7 of Ref. [6]).) In this simple case, the neuron can distinguish between the two sequences by adjusting its threshold h so that it only fires in response to C-B-A. In fact, such a system is a crude form of motion detector. This simple example illustrates how the response of the neuron is sensitive to the ordering of the patterns within a sequence. We shall return to this issue in Sec. V.

To study Eq. (3.7) in more detail, it is useful to express the modified Bessel function I_n in an equivalent integral form so that Eq. (3.4) becomes

$$\chi(\alpha-\beta,t)=\int_{-\pi}^{\pi}\frac{dk}{2\pi}e^{ik(\alpha-\beta)}e^{-t\varepsilon(k)} , \tag{3.9}$$

$$\varepsilon(k)=\frac{1}{\bar{\tau}}+\frac{2}{\gamma}(1-\cos k) . \tag{3.10}$$

Equation (3.9) implies that the Fourier transform of the response function χ is given by $\exp[-t\varepsilon(k)]$; N.B., χ is translation invariant for a uniform, infinite, one-dimensional chain. [Such a result could have been derived directly by noting that (3.1) is the solution to Eq. (2.1) with $I_\alpha=0$ and $V_\alpha(0)=\delta_{\alpha\beta}$, and Fourier transforming (2.1).] It follows from Eqs. (3.7) and (3.9) that

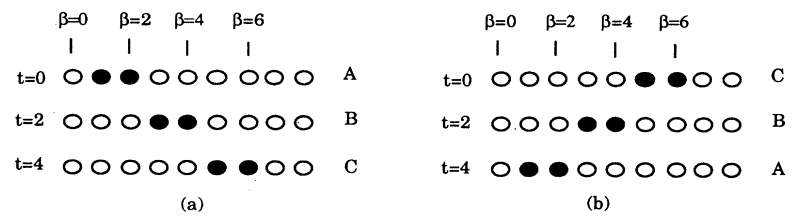

FIG. 6. Sequences of input patterns presented to the model neuron of Sec. III. The time between successive patterns of a sequence is $\Delta t=2$. Compartments stimulated by an input at a particular time are represented by shaded circles. (a) shows a sequence A-B-C in which stimulation proceeds from proximal to distal locations along the positive half of the chain with respect to the soma at $\beta=0$. (b) shows the reverse input sequence C-B-A, with distal compartments stimulated first.

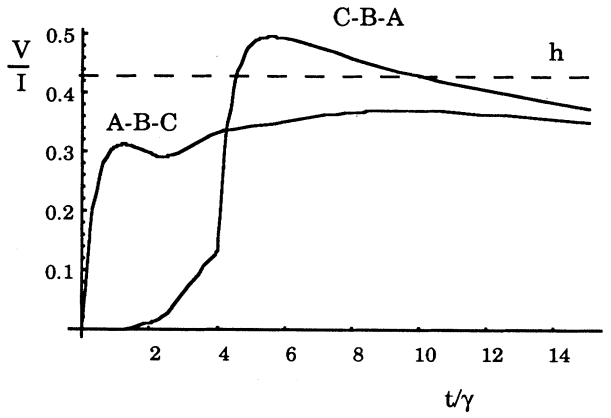

FIG. 7. Response of model neuron to the sequences *A-B-C* and *C-B-A* of Fig. 6. The activation state V is measured in units of I, where I is the effective amplitude of each input pattern.

$$V(t)=\int_0^t ds \int_{-\pi}^{\pi} dk\, e^{-(t-s)\varepsilon(k)} \sum_{\alpha=-\infty}^{\infty} e^{ik\alpha} \mathbf{w}_\alpha \cdot \mathbf{x}_\alpha(s) \ . \tag{3.11}$$

Hence, we may analyze the response of the neuron to a general input by Fourier transforming $\mathbf{w}_\alpha \cdot \mathbf{x}_\alpha(t)$.

Consider, for simplicity, an input of the form $\mathbf{w}_\alpha \cdot \mathbf{x}_\alpha(t)=u(t)\cos p\alpha$, $-\pi \le p \le \pi$, for all α. When $p=0$, every compartment receives the same excitatory $[u(t)>0]$ or inhibitory $[u(t)<0]$ input. On the other hand, when $p=\pi$ and $u(t)>0$, the input to a compartment along the chain alternates between an excitatory one (α even) and an inhibitory one (α odd). For such a choice of inputs, Eq. (3.11) reduces to

$$V(t)=\int_0^t ds\, e^{-(t-s)\varepsilon(p)} u(s) \ , \tag{3.12}$$

which has the equivalent differential form

$$\frac{dV}{dt}=-\varepsilon(p)V(t)+u(t) \ . \tag{3.13}$$

Therefore, in response to an input pattern of a given spatial frequency across the chain, the model neuron is equivalent to a leaky-integrator neuron with decay rate $\varepsilon(p)$ that is frequency dependent. Assuming that $\bar{\tau}$ and γ are of comparable size then there will be a significant contribution to the effective decay rate from the p-dependent term $2(1-\cos p)/\gamma$. (Recall from Eqs. (2.2) and (3.2) that the particular value of γ will depend upon the diameter d and length l of a compartment. On the other hand, $\bar{\tau}$ is a more universal quantity in the sense that it is independent of particular geometry. Typically, $\bar{\tau}$ lies in the range 10–100 ms [7].)

It follows from the above that the output firing rate of a neuron will be p dependent. To illustrate this, we consider a simple *integrate-and-fire* model neuron in which the activation state $V(t)$ satisfies Eq. (3.13) with $u(t)=I$, a constant input, together with the reset condition

$$V(t^+)=0 \ \text{ if } \ V(t)=h \ . \tag{3.14}$$

That is, $V(t)$ is reset to zero whenever the neuron reaches threshold h and fires. [Recall from the derivation of Eqs. (2.16) and (2.17) that we are implicitly assuming that the whole neuron resets its membrane potential on firing.] Solving Eqs. (3.13) and (3.14), the firing times T_n of the neuron satisfy the iterative equation

$$h=\frac{I}{\varepsilon(p)}(1-e^{-\varepsilon(p)(t_{N+1}-t_N)}) \ . \tag{3.15}$$

Assuming that $h\varepsilon(p)<I$ (for all p), then the firing frequency of the neuron is $\eta=(\Delta t)^{-1}$, where

$$\Delta t \equiv t_{N+1}-t_N=-\varepsilon(p)^{-1}\ln[1-h\varepsilon(p)/I] \tag{3.16}$$

Here Δt is a monotonically increasing function of ε such that $\Delta t \approx h/I$ for $\varepsilon \ll I/h$ and $\Delta t \to \infty$ as $\varepsilon \to I/h$. Therefore, the output firing rate of the neuron decreases monotonically as the spatial frequency of the input pattern across the dendritic chain increases from $p=0$ to $p=\pi$.

Another consequence of Eq. (3.16) is that the firing frequency η would increase to $f_{\max}=1/t_R$, where t_R is the absolute refractory period, as the input I increases. Indeed for large I, η is approximately linear in I. This can lead to unrealistically high firing rates in recurrent neural networks; see Sec. IV. Finally, note that one can also analyze the behavior of the neuron for more general choices of $u(t)$. For example, the results of Keener, Hoppenstead, and Rinzel [14] carry over straightforwardly to the case of an oscillatory input of the form $u(t)=I(1+B\cos t)$, where the firing frequency exhibits a more complicated dependence on $\varepsilon(p)$. Extensions to the case of inputs consisting of a mixture of spatial frequencies, however, is nontrivial.

So far in this section we have assumed that the dendritic chain is uniform. An interesting modification of this simple picture is the introduction of nonuniformities representing, for example, the fact that the diameter of dendrites of real neurons tends to decrease distally from the soma. (Indeed, the thinnest branches of the tree, the dendritic spines, are thought to play a central role in dendritic processing [5].) We shall briefly indicate how such a feature may be incorporated into our model in the case of an infinite chain. Using Eqs. (2.2) and (2.8), we set

$$\frac{1}{\tau_\alpha}=\frac{2d(\alpha)}{\gamma}+\frac{1}{\bar{\tau}} \ , \quad \tau_{\alpha\alpha+1}=\frac{\gamma}{d(\alpha)}=\tau_{\alpha+1\alpha} \ , \tag{3.17}$$

where $d(\alpha)$ is a monotonically decreasing function of $|\alpha|$. (Recall that the soma is assumed to be isopotential with the compartment at $\alpha=0$.) We can analyze the effects of this nonuniformity using Fourier methods. The result is that Eq. (3.1) becomes

$$\chi(\alpha,t;\beta,0)=\int_{-\pi}^{\pi}\frac{dp}{2\pi}\int_{-\pi}^{\pi}\frac{dp'}{2\pi}e^{ip\alpha}e^{-ip'\beta}[e^{tQ}]_{pp'} \ , \tag{3.18}$$

where

$$[e^{tQ}]_{pp'}=\sum_{n=0}^{\infty}\frac{t^n}{n!}\left[\prod_{j=1}^{n}\int_{-\pi}^{\pi}dk_j\right]Q_{pk_1}Q_{k_1k_2}\cdots Q_{k_np'}\ , \tag{3.19}$$

$$Q_{kk'}=-\frac{2\pi}{\bar{\tau}}\delta(k-k')-\frac{d_{k-k'}}{\gamma}(2-e^{ik}-e^{ik'})\ ,$$

and d_k is the Fourier transform of the diameter $d(\alpha)$. For a uniform chain, $d_k=\delta(k)$ and (3.18) reduces to (3.9). On the other hand, Eqs. (2.14) and (3.18) imply that in the case of a decreasing diameter, the resulting nonuniformity leads to a "scattering" of input pattern modes, as expressed by the nonzero off-diagonal contributions to the matrix $\exp(t\mathbf{Q})$. The possible effects of tapering dendrites will be investigated elsewhere.

One final point is in order. All the analysis of this section carries over quite straightforwardly in the continuum limit to the case of an infinite dendritic cable. For example, if we introduce a length scale into Eq. (3.9) by specifying the length of each compartment to be l, then in the continuum limit, $l\to 0$, we obtain the response function of an infinite cable satisfying Eq. (2.3). To show this, set $x=\beta l$ and rewrite (3.9) as

$$\chi(x-y,t)=l\int_{-\pi/l}^{\pi/l}\frac{dk}{2\pi}e^{ik(x-y)}e^{-t/\bar{\tau}}\times e^{-2t(1-\cos lk)/\gamma}\ . \tag{3.20}$$

Taking the limit $l\to 0$ and performing the integration over k gives

$$\left[\frac{D}{4\pi t}\right]^{1/2}e^{-t/\bar{\tau}}e^{-D(x-y)^2/4t}\ , \tag{3.21}$$

where $D=\lim_{l\to 0}\gamma/l^2=\bar{\tau}/\lambda^2$. One can then define a neuron model along similar lines to Eq. (3.11). For a discrete set of synapses,

$$V(t)=\int_0^t ds\int_{-\infty}^{\infty}dk\,e^{-(t-s)\varepsilon(k)}\sum_{\alpha}e^{ikx_\alpha}u_\alpha(s)\ , \tag{3.22}$$

where $\varepsilon(k)=\bar{\tau}^{-1}+k^2/D$ and u_α is the net input to the αth synapse located at position x_α along the cable. [Note, however, that the compartmental model response function, Eq. (2.11), is easier to compute than its corresponding continuum version when one considers nonuniform dendritic branching structures rather than a uniform one-dimensional cable. Therefore, to allow for a direct comparison with such computations, it is useful to follow a compartmental approach in the simpler one-dimensional case analyzed in this paper.]

IV. SHUNTING EFFECTS

When shunting effects are taken into account, the resulting solution (2.10) to the compartmental model equations involves a time-ordered path integral, which is difficult to analyze further without making additional assumptions concerning the synaptic inputs. A major simplification occurs if we take the synaptic inputs to be constant. Suppose, for example, that each compartment consists of two groups of identical synapses, one excitatory and the other inhibitory, such that

$$\frac{1}{C_\alpha}\sum_k\Delta g_{\alpha k}(t)=E_\alpha+I_\alpha\ ,$$
$$\frac{1}{C_\alpha}\sum_k S_{\alpha k}\Delta g_{\alpha k}(t)=S_\alpha^{(e)}E_\alpha+S_\alpha^{(i)}I_\alpha\ , \tag{4.1}$$

where E_α and I_α are the constant rates of excitatory and inhibitory stimulation of the αth compartment, and $S_\alpha^{(e,i)}$ are the associated membrane reversal potentials with $S_\alpha^{(e)}>0$ and $S_\alpha^{(i)}\le 0$. Substituting Eq. (4.1) into (2.4), it can be seen that constant synaptic activity in the presence of shunting leads to a time-independent modification of the leakage resistance R_α given by $1/R_\alpha\to 1/R_\alpha+(E_\alpha+I_\alpha)$ such that the matrix $\mathbf{H}$ of (2.6) becomes

$$H_{\alpha\beta}=Q_{\alpha\beta}+(E_\alpha+I_\alpha)\delta_{\alpha\beta}\ . \tag{4.2}$$

Equation (2.4) can then be solved without introducing a time-ordering operator to give the following result for the activation state $V(t)$, corresponding to the membrane potential at the soma [cf. Eq. (2.14)],

$$V(t)=\sum_{\alpha=-M}^{M}(S_\alpha^{(e)}E_\alpha+S_\alpha^{(i)}I_\alpha)\int_0^t ds[e^{-(t-s)\mathbf{H}}]_{0\alpha}\ . \tag{4.3}$$

Hence, in the presence of shunting, the activation state is a nonlinear function of the constant excitatory and inhibitory inputs E_α and I_α, which is manifested as an input-dependent modification of the time constants τ_α of Eq. (2.7).

To illustrate an important consequence of the nonlinear effects of shunting, we shall determine the steady-state value V^∞ of the activation state $V(t)$ in the case of the infinite uniform dendritic chain considered in Sec. III. Suppose that the Lth compartment receives an excitatory input at a constant rate of stimulation E while every other compartment receives inhibitory inputs at a constant rate I (Fig. 8). In other words, $E_\alpha=E\delta_{\alpha L}$, $I_\alpha=I(1-\delta_{\alpha L})$. Assume that the chain is uniform so that Eq. (3.2) holds and $S_\alpha^{(e,i)}=S^{(e,i)}$ for all α. In order that the modifications to the matrix $\mathbf{H}$ of Eq. (4.2) are also uniform, we shall impose the additional condition $E=I$

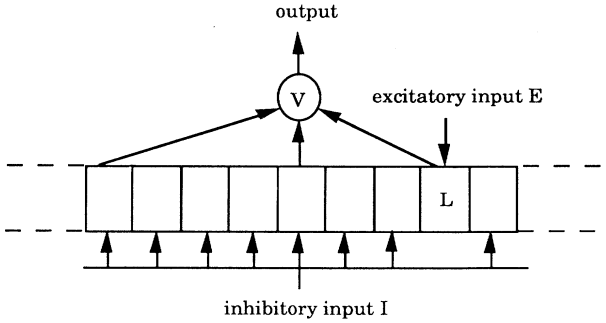

FIG. 8. Pattern of inhibitory and excitatory inputs used to study the effects of shunting on the steady-state behavior of a compartmental model neuron. The Lth compartment receives an excitation at a rate E while all other compartments receive shunting inhibition at a rate I with $I=E$.

so that $H_{\alpha\beta}=Q_{\alpha\beta}+E\delta_{\alpha\beta}$, i.e., there is an input-dependent modification of the membrane potential time constant $\bar{\tau}$ of the form $1/\bar{\tau}\rightarrow 1/\bar{\tau}+E$. We shall also assume that the inhibition is in the form of a *shunting inhibition* [5] by setting $S^{(i)}=0$. In this case the inhibition does not contribute directly to the activation state $V(t)$ but effects its behavior indirectly through the nonlinear dependence on inputs. Under the above simplifications, taking the limit $M\rightarrow\infty$ in Eq. (4.3) gives

$$V(t)=S^{(e)}E\int_0^t ds\, e^{-(t-s)E}\chi(L,t-s)\ , \tag{4.4}$$

where $\chi(L,t)$ is the response function of an infinite, uniform dendritic chain, which was evaluated in Sec. III. Substituting the expression for $\chi(L,t)$, Eq. (3.9), into Eq. (4.4) and performing the resulting time integral,

$$V(t)=S^{(e)}E\int_{-\pi}^{\pi}\frac{dk}{2\pi}\frac{e^{ikL}}{[\varepsilon(k)+E)]}(1-e^{-t[\varepsilon(k)+E]})\ . \tag{4.5}$$

In the limit $t\rightarrow\infty$, the transient term $\exp[-t\varepsilon(k)]$ in Eq. (4.5) vanishes. The resulting expression for the steady-state value of the activation state, V^{∞}, may be rewritten as a contour integral on the unit circle C in the complex plane. That is, introducing the change of variables $z=e^{ik}$ and substituting for $\varepsilon(k)$ using Eq. (3.10),

$$V^{\infty}=S^{(e)}E\oint_C\frac{dz}{2\pi i}\frac{z^L}{(E+\epsilon_0+2\gamma^{-1})z-\gamma^{-1}(z^2+1)}\ , \tag{4.6}$$

where $\epsilon_0=1/\bar{\tau}$. The denominator in the integrand has two roots,

$$\lambda_{\pm}=1+\frac{\gamma(E+\epsilon_0)}{2}\pm\left[\left[1+\frac{\gamma(E+\epsilon_0)}{2}\right]^2-1\right]^{1/2}\ , \tag{4.7}$$

with λ_- lying within the unit circle. Hence

$$V^{\infty}=\gamma S^{(e)}E\frac{(\lambda_-)^L}{\lambda_+-\lambda_-}\ . \tag{4.8}$$

For small levels of excitation E, V^{∞} is approximately a linear function of E. However, as E increases, the contribution of shunting inhibition to the effective decay rate becomes more and more significant so that V^{∞} eventually begins to decrease. Indeed, for large E, $\lambda_+-\lambda_-\approx\gamma E$ and $V^{\infty}\approx S^{(e)}(\lambda_-)^L$, with $\lambda_-\rightarrow 0$ as $E\rightarrow\infty$. This is illustrated in Fig. 9, where $V^{\infty}/S^{(e)}$ is plotted as a function of $\bar{\tau}E$ for $\gamma=0.5\bar{\tau}$ and $L=1$ in Eq. (4.8). (Note that the level of excitation E has units of frequency.)

A cable version of the above analysis may be obtained by taking the continuum limit along similar lines to the derivation of Eq. (3.21). For example, suppose that we have a pattern of excitation $E(x)=E$ for $x\in[L_0,L_1]$ and a pattern of shunting inhibition $I(x)=I$ for $x\notin[L_0,L_1]$, where x is the position from the soma (at $x=0$) along an infinite uniform cable. Setting $E=I$, the continuum limit version of Eq. (4.5) is

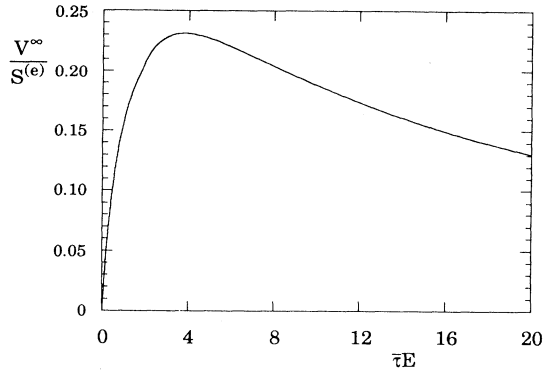

FIG. 9. Stationary activation state V^{∞} (in units of membrane reversal potential $S^{(e)}$) as a function of the excitatory rate of stimulation E (with E^{-1} in units of membrane time constant $\bar{\tau}$) for the input pattern shown in Fig. 8 with $L=1$.

$$V(t)=S^{(e)}E\int_{L_0}^{L_1}dx\int_{-\infty}^{\infty}\frac{dk}{2\pi}\frac{e^{ikx}}{[\varepsilon(k)+E]}\times(1-e^{-t[\varepsilon(k)+E]})\ , \tag{4.9}$$

$$\varepsilon(k)=\frac{1}{\bar{\tau}}+\frac{k^2}{D}\ ,$$

where D is the diffusion constant defined below Eq. (3.21). Evaluating Eq. (4.9) in the limit $t\rightarrow\infty$ gives, for $L_0>0$,

$$V^{\infty}=S^{(e)}\sqrt{D}\frac{E}{\sqrt{E+\epsilon_0}}(e^{-L_0[D(E+\epsilon_0)]^{1/2}}-e^{-L_1[D(E+\epsilon_0)]^{1/2}})\ . \tag{4.10}$$

The general behavior of Eq. (4.10) for fixed L_0 and L_1 is similar to that shown in Fig. 9 for the corresponding compartmental model expression, Eq. (4.8). At low levels of stimulation E, V^{∞} is a linear function of E, whereas for large E, $V^{\infty}\approx S^{(e)}\sqrt{DE}\exp(-L_0\sqrt{DE})$, so that $V^{\infty}\rightarrow 0$ as $E\rightarrow\infty$. It is also interesting to note that the effective characteristic length of the cable is $\lambda\sqrt{\epsilon_0}/\sqrt{E+\epsilon_0}$, which follows from equation (4.10) and the identity $D=\bar{\tau}/\lambda^2=1/\epsilon_0\lambda^2$. (Modifications in the membrane potential time constant and characteristic length of a real neuron have recently been observed in a number of experiments [18].)

An analogous result to Eq. (4.10) has been derived by Abbott [8], who considers solutions to the *stationary* cable equations for a model neuron with the structure of Fig. 3(a). Following Ref. [8], we shall show how the inclusion of shunting inhibition along the above lines can remove the problem of high firing rates that plague recurrent network models based on neurons whose activation states vary linearly with inputs. When such networks are in a state of self-sustained firing, the neurons tend to fire at their maximum rates, whereas real cortical neurons fire well below their maximum rates. Such a problem has received considerable attention within the context of associative memory networks [19]. If we take $f(V(t))$ to be the firing rate of the neuron at time t, with

f given by Eq. (2.13), then the steady-state firing rate is

$$f(E)=\frac{f_{\max}}{1+e^{-g[V^{\infty}(E)-\kappa]}}\ , \tag{4.11}$$

where V^{∞} satisfies Eq. (4.8). [For simplicity, we shall consider the compartmental model version, although the analysis applies equally well in the case of a continuous cable, Eq. (4.10).]

Consider a population of excitatory neurons in which the effective excitatory rate E impinging on a neuron is determined by the average firing rate $\langle f \rangle$ of the population. Similarly, the inhibitory rate F is determined by the average firing rate of a population of inhibitory interneurons. For a large population of neurons, a reasonable approximation is to take $E=c\langle f \rangle$, for some constant c. Within a mean-field approach, the steady-state behavior of the population is then determined by the self-consistency condition $E=cf(E)$ [8]. Using graphical methods, one finds that there are two stable solutions to this equation, one corresponding to the silent state $E=0$ and the other to a state in which the firing rate is considerably below $f_{\max}$. This is illustrated by curve (b) of Fig. 10, where $f/f_{\max}$, satisfying Eq. (4.11) with $cf_{\max}=1, g^{-1}=0.03$, and $\kappa=0.25$, is plotted as a function of $\bar{\tau}E$ for V^{∞} given by Eq. (4.8) with $\gamma=0.5\bar{\tau}$. (Note that there is a third solution to the self-consistency condition but this is unstable.) On the other hand, in the absence of shunting, V^{∞} is a linear function of E, i.e., E is set to zero in the definition of $\lambda_{\pm}$ in (4.7). Then the nonsilent stable state has a firing rate close to $f_{\max}$; see curve (a) of Fig. 10. (We have followed the proof of Ref. [8].)

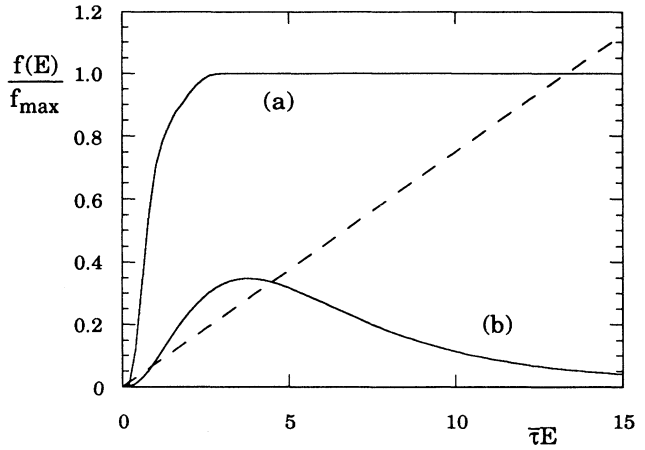

FIG. 10. Firing-rate/maximum firing-rate $f/f_{\max}$ as a function of input excitation E for (a) linear and (b) nonlinear relationships between stationary activation state V^{∞} and E. Points of intersection with straight line are states of self-sustained firing.

A straightforward generalization of the pattern of stimulation shown in Fig. 8 is to assume that each compartment α has an excitatory input E_{α} and an inhibitory input $I_{\alpha}=\sum_{\beta\neq\alpha}E_{\beta}$. In other words, each input E_{α} excites compartment α and inhibits all other compartments, $\beta\neq\alpha$. (This is known as nonrecurrent lateral inhibition [7].) Equation (4.8) then becomes

$$V^{\infty}=\gamma S^{(e)}\sum_{\alpha}E_{\alpha}\frac{(\lambda_{-})^{|\alpha|}}{\lambda_{+}-\lambda_{-}}\ ,$$

where $\lambda_{\pm}$ satisfies Eq. (4.7) with $E=\sum_{\alpha}E_{\alpha}$. (We have assumed that $S^{(i)}=0$ as before.) Since $\lambda_{-}<1$, the effective contribution from an input E_{α} decreases as $|\alpha|$ increases, i.e., as one proceeds from proximal to distal locations along the dendritic chain. This feature is enhanced when the total stimulation E is increased due to the fact that λ_{-} is a monotonically decreasing function of E. Indeed, $V^{\infty}\to\gamma E_0/E$ when $E\to\infty$.

So far, we have considered shunting in the special case of constant synaptic inputs such that the time-ordering operator of Eq. (2.10) is no longer required. We now show how Eq. (2.10) can also be analyzed for time-dependent synaptic inputs, provided that we make a number of simplifying assumptions concerning the nature of these inputs: (i) each action potential and postsynaptic potential is idealized as a Dirac δ-function spike, i.e., details of pulse shape are neglected, and (ii) the arrival times of the action potentials are restricted to be integer multiples of a fundamental unit of time t_D. The time-varying conductance $\Delta g_{\alpha k}(t)$, Eq. (2.5), induced by an incoming stream of action potentials is then a sequence of conductance spikes of the form

$$\Delta g_{\alpha k}(t)=\epsilon_{\alpha k}\sum_{m\geq 0}\delta(t-mt_D)a_{\alpha k}(m)\ , \tag{4.12}$$

where $a_{\alpha k}(m)=1$ if an action potential arrives at the discrete time mt_D and is zero otherwise. Substituting Eq. (4.12) into (2.9) we obtain

$$\begin{aligned}\bar{Q}_{\alpha\beta}(t)&=-\delta_{\alpha\beta}\sum_{m\geq 0}\delta(t-mt_D)\mathbf{J}_{\alpha}\cdot\mathbf{a}_{\alpha}(m)\ ,\\ U_{\alpha}(t)&=\sum_{m\geq 0}\delta(t-mt_D)\mathbf{w}_{\alpha}\cdot\mathbf{a}_{\alpha}(m)\ ,\end{aligned} \tag{4.13}$$

where $w_{\alpha k}=\epsilon_{\alpha k}S_{\alpha k}/C_{\alpha}$ and $J_{\alpha k}=\epsilon_{\alpha k}/C_{\alpha}$. Hence, we effectively have two related sets of weights, with $J_{\alpha k}\propto|w_{\alpha k}|$.

The important feature of the expression for the conductance changes in Eq. (4.12) is that the presence of Dirac δ functions allows the integrals in (2.10) to be performed explicitly. More specifically, substituting (4.13) into (2.10) with $t_D=1$, and setting $\mathbf{V}(0)=0$, we obtain for noninteger times t,

$$V_{\alpha}(t)=\sum_{\beta\in J}\sum_{n=0}^{[t]}\mathbf{T}\left\{\exp\left[\int_{n}^{t}dt'\left[\mathbf{Q}-\sum_{p\geq 0}\mathbf{G}(p)\delta(t'-p)\right]\right]\right\}_{\alpha\beta}\mathbf{w}_{\beta}\cdot\mathbf{a}_{\beta}(n)\ , \tag{4.14}$$

where $[t]$ denotes the largest integer $m \leq t$, $G_{\alpha\beta}(p)=\delta_{\alpha\beta}\mathbf{J}_\alpha(p)\cdot\mathbf{a}_\alpha(p)$. The time-ordered product in (4.14) may be evaluated by splitting the interval $[n,[t]]$ into LT equal partitions $[t_i,t_{i+1}]$, where $T=[t]-n, t_0=n, t_L=n+1,\ldots,t_{LT}=[t]$, such that $\delta(t-s)\rightarrow\delta_{i,Ls}/L$. In the limit $L\rightarrow\infty$, we obtain

$$V_\alpha(t)=\sum_{n=0}^{[t]}\sum_\beta \chi(\alpha,t;\beta,n)\mathbf{w}_\beta\cdot\mathbf{a}_\beta(n)\ , \tag{4.15}$$

where χ is the response function

$$\chi(\alpha,t;\beta,n)=[(e^{(t-[t])\mathbf{Q}}e^{-\mathbf{G}([t])} \times e^{\mathbf{Q}}e^{-\mathbf{G}([t]-1)}\ldots e^{\mathbf{Q}}e^{-\mathbf{G}(n)})_{\alpha\beta}]\ . \tag{4.16}$$

Equation (4.15) may be rewritten as

$$V_\alpha(t)=\sum_\beta (e^{(t-m)\mathbf{Q}})_{\alpha\beta}X_\beta(m)\ ,\quad m<t<m+1\ , \tag{4.17}$$

where X_β satisfies

$$X_\alpha(m)=\sum_\beta\sum_{n=0}^{m}\chi(\alpha,m;\beta,n)\mathbf{w}_\beta\cdot\mathbf{a}_\beta(n)\ . \tag{4.18}$$

Since $(\exp\mathbf{Q})_{\alpha\beta}$ is a smooth function of t such that $(\exp\mathbf{Q})_{\alpha\beta}\rightarrow\delta_{\alpha\beta}$ in the limit $t\rightarrow 0$, we can approximate $V_\alpha(t)$ in the interval $m<t<m+1$ by $X_\alpha(m)$ provided that t_D is sufficiently small. Thus we effectively have a discrete-time compartmental model neuron in which the output at the mth time step is $f(V(m))$, where [cf. Eq. (2.14)]

$$V(m)=\sum_{n=0}^{m}\chi_\alpha(m,n)\mathbf{w}_\alpha\cdot\mathbf{a}_\alpha(n)\ , \tag{4.19}$$

$$\chi_\alpha(m,n)=(e^{-\mathbf{G}(m)}e^{\mathbf{Q}}e^{-\mathbf{G}(m-1)}e^{\mathbf{Q}}\ldots e^{\mathbf{Q}}e^{-\mathbf{G}(n)})_{0\alpha}\ . \tag{4.20}$$

In this example, shunting leads to the insertion of the factors $\exp[-\mathbf{G}(p)]$ so that the response function χ_α is no longer time-translation invariant, i.e., it is not simply a function of m-n, and it is input dependent. Since the weights $\mathbf{J}_\alpha$ are positive valued, the factors $\exp[-\mathbf{G}(p)]$ tend to reduce the response of the neuron relative to the case without shunting. In the special case of a single compartment ($M=0$),

$$V(m)=\sum_{n=0}^{m}\exp(-m/\bar{\tau})\exp[-\mathbf{J}\cdot\mathbf{N}(m,n)]\mathbf{w}\cdot\mathbf{a}(n)\ , \tag{4.21}$$

where $N_k(m,n)=a_k(m)+a_k(m-1)+\ldots+a_k(n)$, which is the number of action potentials received by the kth of the neuron in the interval $[m,n]$.

Equations (4.20) and (4.21) can be considered as single-compartmental and multicompartmental versions of the standard discrete-time model of a neuron [15] in which shunting effects are included. It would be of interest to determine how the dynamical, statistical mechanical and information processing properties of discrete-time networks are modified when shunting and/or compartmental structure is taken into account along the above lines. For example, one of the consequences of shunting is the existence of two related sets of weights $J_{\alpha k}$ and $w_{\alpha k}$, both of which are proportional to the synaptic efficacies $\epsilon_{\alpha k}$ of Eq. (2.5). Since learning involves a modification of $\epsilon_{\alpha k}$, rather than $S_{\alpha k}$, this implies that both sets of weights are altered during learning. Another issue concerns the possibility of the weights $J_{\alpha k}$ taking negative values; this corresponds to an input inducing a decrease rather than an increase in the conductance $\Delta g_{\alpha k}$ of Eq. (2.4). (Such a process can occur in real neurons [5].) Under such circumstances, the nonlinear input-dependent factors in Eqs. (4.20) and (4.21) may lead to chaotic dynamics as signaled by the presence of positive Liapunov exponents [20]. We hope to consider these various issues in more detail elsewhere.

V. TEMPORAL SEQUENCE PROCESSING

Recall from the example of Sec. III, Figs. 6 and 7, that the model neuron constructed in Sec. II can extract temporal features of an input sequence such as the ordering of patterns within that sequence. In this section, we consider this issue in more detail by extending recent work on temporal processing in time-summating neurons [9]. First, note that an important property of the compartmental model neuron from the viewpoint of temporal processing is that the activation state $V(t)$ of Eq. (2.14) develops an internal representation of input history that allows the neuron to operate directly in the time domain. Such a representation is determined by the response functions χ_α and may be treated in two different ways [17,21]. The first approach is to consider the χ_α as basis functions for a set of time-dependent weights. In particular, suppose that the same input is presented to all compartments, $x_{\alpha k}=x_k$ for all α. Then Eq. (2.14) may be rewritten as

$$\begin{aligned} V(t)&=\sum_{j=1}^{N}\int_0^t ds\, w_j(t-s)x_j(s)\ ,\\ w_j(t)&=\sum_\alpha \chi_\alpha(t)w_{\alpha j}\ , \end{aligned} \tag{5.1}$$

so that the neuron consists of N time-dependent weights $w_j(t)$, which are expanded in terms of the basis functions χ_α. The alternative approach, which is more in keeping with the neuron model illustrated in Fig. 4, is to consider the χ_α as filters that transform the inputs $x_{\alpha k}(t)$ into a new set $z_{\alpha k}(t)$ with the weights $w_{\alpha k}$ fixed. In other words, Eq. (2.14) is rewritten in the form

$$\begin{aligned} V(t)&=\sum_{j=1}^{N}\sum_\alpha w_{\alpha j}z_{\alpha j}(t)\ ,\\ z_{\alpha j}(t)&=\int_0^t\chi_\alpha(t-s)x_{\alpha j}(s)\ . \end{aligned} \tag{5.2}$$

(If χ_α satisfies Eq. (3.5), then Eq. (5.2) reduces to the gamma model of Ref. [17].) The usefulness of the latter formulation is that one can interpret the operation of the model neuron in terms of a perceptron and apply well-known results on perceptron learning [22].

Consider, for sake of illustration, a discrete-time ver-

sion of Eq. (5.2) given by

$$V(m)=\sum_{\alpha=-M}^{M}\mathbf{w}_\alpha\cdot\mathbf{z}_\alpha(m)\ ,$$
$$z_{\alpha k}(m)=\sum_{n=1}^{m}\chi_\alpha(m-n)a_{\alpha k}(n)\ , \tag{5.3}$$

where $\chi_\alpha(m)=[e^{m\mathbf{Q}}]_{0\alpha}$, $\mathbf{Q}$ satisfies Eq. (2.7), and $\mathbf{a}_\beta=(a_{\beta k},k=1,\ldots,N)$, with $a_{\beta k}=0,1$. [Equation (5.3) is equivalent to Eq. (4.19) in the absence of shunting, with $a_{\alpha k}(m)$ determining whether or not an action potential arrives at the kth synapse of the αth compartment at time m.] The output of the neuron is taken to be binary valued, $f(V(m))=\theta(V(m)-h)$, where $\Theta(x)=1$ if $x>0$ and 0 otherwise. In the case $M=0$, Eq. (5.3) describes a time-summating neuron

$$V(m)=\sum_{k=1}^{N}w_k z_k(m)\ ,\quad z_k(m)=\sum_{n=1}^{m}d^{m-n}a_k(n)\ , \tag{5.4}$$

where $d=e^{-1/\tau}$. The activation state is given by a decaying activity trace of previous inputs to the neuron.

Following Ref. [9], we shall first construct versions of the perceptron learning rule and convergence theorem [22] for a time-summating neuron and use geometrical methods to study how such neurons can resolve ordering and coarticulation effects arising in temporal sequences. In particular, suppose that a time-summating neuron is required to learn p input-output mappings $\{\mathbf{A}^\mu(m);m=1,\ldots,T\}\to\{\tilde{a}^\mu(m),\quad m=1,\ldots,T\},\mu=1,\ldots,p$. Define a new set of inputs of the form $\mathbf{Z}^\mu(m)=(z_1^\mu(m),\ldots,z_N^\mu(m)),\mu=1,\ldots,p,m=1,\ldots,T$ where each z_j^μ satisfies

$$z_k^\mu(m)=\sum_{n=1}^{m}d^{m-n}a_k^\mu(n)\ . \tag{5.5}$$

Divide the pT inputs $\mathbf{Z}^\mu(m)$ into two sets F^+ and F^-, where $\mathbf{Z}^\mu(m)\in F^+$ if $\tilde{a}^\mu(t)=1$ and $\mathbf{Z}^\mu(m)\in F^-$ otherwise. Learning then reduces to the problem of finding a set of weights $\{w_k,k=1,\ldots,N\}$ such that the sets F^+ and F^- are separated by a single hyperplane in the space of inputs $\mathbf{Z}^\mu(m)$-linear separability. In other words, the weights must satisfy the pT conditions

$$\sum_{j=1}^{N}w_j z_j^\mu(m)>h+\delta\quad\text{if }\mathbf{Z}^\mu(m)\in F^+\ ,$$
$$\sum_{j=1}^{N}w_j z_j^\mu(m)<h-\delta\quad\text{if }\mathbf{Z}^\mu(m)\in F^- \tag{5.6}$$

for some $\delta>0$. The perceptron convergence theorem [22] for a time-summating neuron may be stated as follows [9]: Suppose that the weights are updated according to the perceptron learning rule

$$w_j\to w_j+\left[\tilde{a}^\mu(m)-\Theta\left[\sum_k w_k z_k^\mu(m)-h\right]\right]z_j^\mu(m) \tag{5.7}$$

If there exists a set of weights that satisfy Eq. (5.6) for some $\delta>0$, then the perceptron learning rule (5.7) will arrive at a solution of (5.6) in a finite number of time steps—independent of N.

The above result implies that a time-summating neuron can learn the set of mappings $\{\mathbf{A}^\mu(m);m=1,\ldots,T\}\to\{\tilde{a}^\mu(m),t=1,\ldots,T\},\mu=1,\ldots,p$ provided that the associated classes F^+ and F^- are linearly separable. We shall illustrate this with a simple example for $N=2$ [9]. Define the vectors $\mathbf{A}=(1,0)^t$, $\mathbf{B}=(0,1)^t$ and consider the input-output sequences **A-B**$\to$1-0 and **B-A**$\to$0-0. This is essentially an ordering problem, since the pattern **A** produces the output 1 or 0 depending, respectively, on whether it precedes or proceeds the pattern **B**. (Thus it could not be solved by a standard perceptron.) We introduce the four vectors

$$\mathbf{Z}^1(1)=\begin{bmatrix}1\\0\end{bmatrix}\ ,\quad \mathbf{Z}^1(2)=\begin{bmatrix}d\\1\end{bmatrix}\ ,$$

$$\mathbf{Z}^2(1)=\begin{bmatrix}0\\1\end{bmatrix}\ ,\quad \mathbf{Z}^2(2)=\begin{bmatrix}1\\d\end{bmatrix}\ .$$

It is clear that the sets $F^+=\{\mathbf{Z}^1(1)\}$ and $F^-=\{\mathbf{Z}^1(2),\mathbf{Z}^2(1),\mathbf{Z}^2(2)\}$ are linearly separable [Fig. 11(a)] and, hence, that the network can learn the above mappings. (On the other hand, the mappings **A-B**$\to$1-1 and **B-A**$\to$0-0 cannot be linearly separated by a single line [Fig. 11(b)], and a multilayer network of time-summating neurons is required [9].)

We note that networks of time-summating neurons, which are also referred to as context units or neurons with local positive feedback, have been applied successfully to problems such as the classification of speech signals [23], motion detection [24], and the storage and recall of temporal sequences [9,25]. However, a major limitation of such networks is that the representation of the temporal structure of previous inputs, Eq. (5.4), is restricted to a decaying sum in which most recent inputs are weighted more heavily than previous ones. This suggests that one advantage of using a compartmental model neuron, as given by Eq. (5.3) for $M>0$, is that the response functions χ_α, $\alpha\neq0$ are described by response

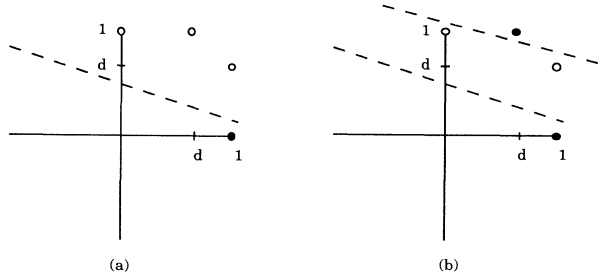

FIG. 11. Example of (a) separable and (b) nonseparable sets F^+ and F^- associated with the sequences of input-output mappings defined in the text. Points in F^+ and F^- are denoted, respectively, by ● and ○.

curves of the form shown in Fig. 5, thus allowing for a more flexible representation of input history. To illustrate this, we shall assume for simplicity that each compartment has a single synapse. We may then view the compartmental model neuron as a perceptron with $2M+1$ input lines with corresponding weights w_β, $\beta=-M,\ldots,M$. In an analogous fashion to the single compartmental neuron, we define a new set of inputs $\mathbf{Z}^\mu(m)$ of the form

$$z_\beta^\mu(m)=\sum_{r=1}^{m}(e^{(m-r)\mathbf{Q}})_{0\beta}a_\beta^\mu(r)\ . \tag{5.8}$$

Defining the sets $F^\pm$ as before, Eqs. (5.6) and (5.7) then hold with the k summation replaced by a β summation. For example, the learning rule (5.7) becomes

$$w_\beta\rightarrow w_\beta+\left[\bar{a}^\mu(m)-\Theta\left[\sum_\alpha w_\alpha z_\alpha^\mu(m)-h\right]\right]z_\beta^\mu(m)\ . \tag{5.9}$$

As a simple example, suppose that the neuron is required to learn the mapping **A-A-A**$\rightarrow$1-0-1, where **A** is defined according to $a_\beta=\delta_{\beta,1}+\delta_{\beta,2}$. Thus, we need only worry about the input lines $\alpha=1,2$. Using Eq. (5.8), we introduce the inputs $\mathbf{Z}(m)$, $m=1-3$, where $z_\beta(1)=a_\beta$, $z_\beta(2)=a_\beta[1+\chi_\beta(1)]$, $z_\beta(3)=a_\beta[1+\chi_\beta(1)+\chi_\beta(2)]$. As shown in Fig. 12, the equivalent perceptron can separate the two classes $F^\pm$ due to the fact that $\chi_1(n)$ and $\chi_2(n)$ are linearly independent functions of n (refer to Fig. 5).

Temporal sequence processing in a compartmental model neuron will be developed further elsewhere [21], in particular, by extending the analysis of the gamma model in Ref. [17]. We conclude this section with a number of comments. First, note that the response function χ_α, in either the discrete-time or continuous-time versions of our model neuron, Eqs. (5.2) and (5.3), is determined by the matrix $\mathbf{Q}$ of Eq. (2.7). It follows from our analysis in Sec. IV that constant background shunting inhibition can modulate the response functions χ_α by changing the effective membrane time constants τ_α that parametrize $\mathbf{Q}$. In other words, shunting inhibition could provide a mechanism for altering the effective memory time span, etc. of the temporal representation of input history. Second, recall that in our treatment of reset at the end of Sec. II we assumed that the membrane potentials of all compartments are reset to zero whenever the neuron fires. This would imply that all information concerning previous inputs is then wiped out. However, a more realistic scenario is that the effects of reset decrease considerably as one proceeds distally from the soma so that at least distal dendrites maintain activity traces over extended periods. This feature can be handled by keeping the transient term $[\exp(t-T_n)\mathbf{Q}]\mathbf{V}(T_n^+)$ in Eq. (2.15), although one can no longer characterize the behavior of the neuron solely in terms of the activation state $V(t)$, as in Eqs. (2.16) and (2.17); one must also explicitly include details concerning the membrane potentials of the individual compartments, V_α, $\alpha\neq 0$.

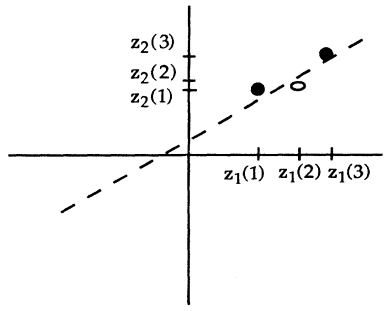

FIG. 12. The sets F^+ and F^- associated with the mapping A-A-$A\rightarrow$1-0-1, where A is given by $a_\beta=\delta_{\beta,1}+\delta_{\beta,2}$

VI. DISCUSSION

In this paper, we have constructed a neural-network model that includes details concerning the passive membrane properties of a neuron's dendrites, and have analyzed the output response of the model to synaptic input patterns. The main results of our analysis are the following:

(i) A compartmental model of passive dendritic processing can be reformulated as a neural-network model in which the activation state of the neuron is of the general form $V(t)=\sum_j\int\chi_j(t,s)w_ja_j(s)ds$, where w_j is the weight of the jth input line, $a_j(s)$ is the input at time s, and χ_j is a response function that incorporates details concerning the dendrites.

(ii) In the case of an infinite, one-dimensional dendritic chain one can derive a simple analytical expression for the response function of the neuron. In particular, one finds that for an input pattern of specific spatial frequency k across the chain, the model neuron is equivalent to a leaky-integrator neuron with effective decay rate $\varepsilon(k)=a+b(1-\cos k)$, a and b positive constants.

(iii) The activation state of the neuron forms an internal representation of an input sequence, thus allowing the neuron to extract temporal features such as the ordering of patterns within the sequence. One of the advantages of taking into account dendritic structure is that it allows for a more flexible representation of input history than given by the decaying activity traces of time-summating neurons, for example. A version of the perceptron learning rule and convergence theorem can be constructed and, at least in simple cases, geometrical methods used to study the ability of the neuron to resolve temporal features of an input sequence.

(iv) The activation state of the model neuron is a nonlinear function of the inputs when shunting effects are taken into account. At the network level shunting inhibition can lead to states of self-sustained firing in which the individual neurons have low firing rates. Shunting inhibition could also provide a mechanism for modulating the internal representation of temporal input history discussed in (iii).

In conclusion, the model neuron constructed in this paper should be of interest both to artificial neural-network modelers and to those involved with real neurons. For the first group, the model neuron is in a form suitable for inclusion as a processing element in a neural network;

the addition of compartmental structure can lead to enhanced temporal discrimination features. In the case of the latter group, our analytical expressions for compartmental neurons contain sufficient detail concerning the properties of real neurons to allow comparison with experimental results *and* to provide insight into principle features of neuronal information processing; some of these features have been specified in (i)–(iv) above. One example where our analysis might be usefully employed is the microcircuitry of Ref. [26].

Note added in proof. The construction of the Green's function for a uniform one-dimensional chain of compartments can be extended to the case of an arbitrary dendritic topology by considering random walks on trees. The resulting expressions reduce to the path integrals of cable theory [27] in the continuum limit.

[1] W. Rall, Exp. Neurol. **2**, 503 (1959).
[2] J. J. J. B. Jack, D. Noble, and R. W. Tsein, *Electrical Current Flow in Excitable Cells* (Clarendon, Oxford, 1975).
[3] C. Koch, T. Poggio, and V. Torre, Proc. Nat. Acad. Sci. USA **80**, 2799 (1983).
[4] J. P. Miller, W. Rall, and J. Rinzel, Brain Res. **325**, 325 (1985); G. M. Shepherd and R. K. Brayton, Neuroscience **21**, 151 (1987).
[5] *The Synaptic Organization of the Brain,* edited by G. M. Shepherd (Oxford University, New York, 1992).
[6] W. Rall, in *Neural Theory and Modeling,* edited by R. F. Reiss (Stanford University, Stanford, 1964), pp. 73–97.
[7] *Methods in Neural Modeling,* edited by C. Koch and I. Segev (MIT, Cambridge, MA, 1989).
[8] L. F. Abbott, Network, **2**, 245 (1991).
[9] P. C. Bressloff and J. G. Taylor, J. Phys. A **26**, L165 (1992).
[10] D. H. Perkel, B. Mulloney, and R. W. Budelli, Neuroscience **6**, 823 (1981).
[11] P. C. Bressloff and J. G. Taylor, Neural Networks **4**, 789 (1991).
[12] W. S. McCulloch and W. Pitts, Bull. Math. Biophys. **5**, 115 (1943).
[13] S. Amari, IEEE Trans. Syst. Man Cybern. **2**, 643 (1972).
[14] B.W. Knight, J. Gen. Phys. **59**, 734 (1972); J. P. Keener, F. C. Hoppenstead, and J. Rinzel, Siam. J. Appl. Math. **41**, 503 (1981).
[15] P. Peretto, *An Introduction to Neural Network Modeling* (Cambridge University, Cambridge, 1992).
[16] G. Grimmett and D. Stirzaker, *Probability and Random Processes* (Clarendon, Oxford, 1982).
[17] B. de Vries and J. C. Principe, Neural Networks **5**, 565 (1992).
[18] O. Bernander, R. J. Douglas, A. C. Martin, and C. Koch, Proc. Nat. Acad. Sci. USA **88**, 11 569 (1991); M. Rapp, Y. Yarom, and I. Segev, Neural Computation **4**, 518 (1992).
[19] D. J. Amit and A. Treves, Proc. Nat. Acad. Sci., USA **86**, 7671 (1989); A. Treves and J. Amit, J. Phys. A **22**, 2205 (1989); N. Rubin and H. Sompolinsky, Europhys. Lett. **10**, 465 (1989).
[20] P. C. Bresssloff, Phys. Rev. A **44**, 4005 (1991).
[21] P. C. Bressloff (unpublished).
[22] M. Minsky and S. Papert, *Perceptrons* (MIT, Cambridge, MA, 1986).
[23] M. C. Mozer, Complex Systems **3**, 349 (1989); P. Frasconi, M. Gori, and G. Soda, Neural Computation **4**, 120 (1992).
[24] W. S. Stornetta, T. Hogg, and B. A. Huberman, in *Neural Information Processing Systems,* edited by D. Anderson (AIP, New York, 1988), pp. 750–759.
[25] M. Reiss and J. G. Taylor, Neural Networks **4**, 773 (1991).
[26] R. J. Douglas and K. A. Martin, J. Physiol. **440**, 735 (1991).
[27] L. F. Abbott, E. Farhi, and S. Gutmann, Biol. Cybern. **66**, 49 (1991).